Available online at www.sciencedirect.com
SCIENCE DIRECT
Tetrahedron
ELSEVIER
Tetrahedron 60 (2004) 9139–9148

Ring transformation of cyclohepta[*b*]pyrimido[5,4-*d*]furan-8(7*H*),10(9*H*)-dionylium ion to the corresponding pyrrole derivatives via troponeimine intermediates: photo-induced autorecycling oxidizing reactions of some amines

Shin-ichi Naya and Makoto Nitta*

Department of Chemistry, School of Science and Engineering, Waseda University, Shinjuku-ku, Tokyo 169-8555, Japan

Received 7 July 2004; revised 26 July 2004; accepted 26 July 2004

Available online 26 August 2004

Abstract—Ring transformation of 7,9-dimethylcyclohepta[*b*]pyrimido[5,4-*d*]furan- 8(7*H*),10(9*H*)-dionylium tetrafluoroborate $\mathbf{4}^+\cdot\mathbf{BF}_4^-$ to 7,9-dimethylcyclohepta[*b*]pyrimido[5,4-*d*]pyrrrole-8(7*H*),10(9*H*)-dionylium tetrafluoroborate $\mathbf{6a–d}^+\cdot\mathbf{BF}_4^-$ consists of the reaction of $\mathbf{4}^+\cdot\mathbf{BF}_4^-$ with amines and subsequent exchange of the counter-ion using aq. HBF_4. Reactions of $\mathbf{4}^+\cdot\mathbf{BF}_4^-$ with aniline and 4-substituted anilines afforded the corresponding pyrrole derivatives $\mathbf{6a–c}^+\cdot\mathbf{BF}_4^-$ directly in good yields. On the other hand, reaction of $\mathbf{4}^+\cdot\mathbf{BF}_4^-$ with benzylamine gave the troponeimine intermediate **9**, which was not converted to $\mathbf{6d}^+\cdot\mathbf{BF}_4^-$ and reverted to $\mathbf{4}^+\cdot\mathbf{BF}_4^-$ by adding HBF_4; however, it was converted to $\mathbf{6d}^+\cdot\mathbf{BF}_4^-$ upon treatment with $(COCl)_2$ or $SOCl_2$, followed by exchange of the counter-ion. In a search for the characteristics of **9**, inspection and comparison of the X-ray crystal analyses, NMR and UV–vis spectra, and CV measurement of **9** and N,N-disubstituted troponeimine derivatives **12** were carried out to suggest the remarkable structure of **12** having ionic C–O bonding between the imine–carbon atom and the oxygen atom of the barbituric acid moiety in the solid state. Thus, characteristics of **9** were ascribed to the sterically hindered and favorable conformation of N-protonated troponeimine intermediates. Furthermore, novel photo-induced oxidation reactions of a series of $\mathbf{4}^+\cdot\mathbf{BF}_4^-$, $\mathbf{5}^+\cdot\mathbf{BF}_4^-$, and $\mathbf{6a,e}^+\cdot\mathbf{BF}_4^-$ towards some amines under aerobic conditions were carried out to give the corresponding imines in 455–8362% yields [based on compounds $\mathbf{4}^+$, $\mathbf{5}^+$, and $\mathbf{6a,e}^+$], suggesting the oxidation reaction occurs in an autorecycling process. Mechanistic aspects of the amine-oxidation reaction are also postulated.

1. Introduction

Flavins are known to play an important role as cofactors in a wide variety of biological redox reactions.[1] Dehydrogenation reactions represent a major category of processes mediated by a subclass of flavoenzymes known as oxidases. Included in this group are the oxidative transformations of alcohols to carbonyl compounds, of amines to imines, and of fatty acid esters to their α,β-unsaturated analogs.[2] The flavin-redox systems have been investigated extensively through synthetic model systems and theoretical calculations.[3] Among these, 5-deazaflavin **1a** (Fig. 1) has been studied extensively in both enzymatic[4] and model systems,[5,6] in the hope of gaining mechanistic insight into flavin-catalyzed reactions. In this relation, 5-deaza-10-oxaflavin **1b** (2*H*-chromeno[2,3-*d*]pyrimidine-2,4(3*H*)-dione),[7] in

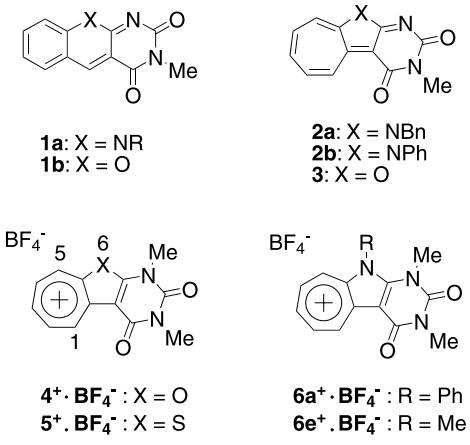

Figure 1.

Keywords: 7,9-Dimethylcyclohepta[*b*]pyrimido[5,4-*d*]furan-8(7*H*),10(9*H*)-dionylium tetrafluoroborate; 7,9-Dimethylcyclohepta[*b*]pyrimido[5,4-*d*]pyrrol-8(7*H*),10(9*H*)-dionylium tetrafluoroborate; Ring-transformation; Photo-induced oxidation reaction.

* Corresponding author. Tel.: +81-352863236; fax: +81-332082735; e-mail: nitta@waseda.jp

0040–4020/$ - see front matter © 2004 Elsevier Ltd. All rights reserved.
doi:10.1016/j.tet.2004.07.063

which the nitrogen atom is replaced by an oxygen, has also been synthesized and found to possess a strong function to oxidize alcohols to the corresponding carbonyl compounds. On the basis of the above observations, we have previously studied the preparation of 6-substituted 9-methylcyclohepta[*b*]pyrimido[5,4-*d*]pyrrole-8(6*H*),10(9*H*)-diones (**2a**,**b**)[8] and 9-methylcyclohepta[*b*]pyrimido[5,4-*d*]furan-8,10(9*H*)-diones (**3**),[9] which are structural isomers of 5-deazaflavin **1a** and 5-deaza-10-oxaflavin **1b**. Furthermore, we have recently reported the synthesis, properties, and reactivity of 7,9-dimethylcyclohepta[*b*]pyrimido[5,4-*d*]furan-8(7*H*),10(9*H*)-dionylium tetrafluoroborate ($\mathbf{4}^+\cdot\mathbf{BF}_4^-$)[11,12] and its sulfur and nitrogen analogues $\mathbf{5}^+\cdot\mathbf{BF}_4^-$ and $\mathbf{6a,e}^+\cdot\mathbf{BF}_4^-$.[13,14] In addition, novel photo-induced autorecycling oxidizing reactions of $\mathbf{4}^+\cdot\mathbf{BF}_4^-$, $\mathbf{5}^+\cdot\mathbf{BF}_4^-$, $\mathbf{6a,e}^+\cdot\mathbf{BF}_4^-$ toward some alcohols are studied as well.[12–14] Thus, the uracil-annulated heteroazulenes such as $\mathbf{4}^+\cdot\mathbf{BF}_4^-$, $\mathbf{5}^+\cdot\mathbf{BF}_4^-$, $\mathbf{6a,e}^+\cdot\mathbf{BF}_4^-$ are very interesting from the viewpoint of exploration of novel functions. Through these studies, we have accomplished a ring-transformation of **3** to **2a**,**b**,[10] which are clarified to have oxidizing ability toward some amines: the reaction of **3** with some amines undergoes ring-opening reaction of furan to give troponimine intermediates which undergo thermal ring-closure to give **2**.

From this viewpoint, we studied the ring transformation of $\mathbf{4}^+\cdot\mathbf{BF}_4^-$ to the corresponding pyrrole derivatives **6a**–$\mathbf{d}^+\cdot\mathbf{BF}_4^-$. In order to clarify the reactivity of the troponeimine intermediate, the detailed structural features

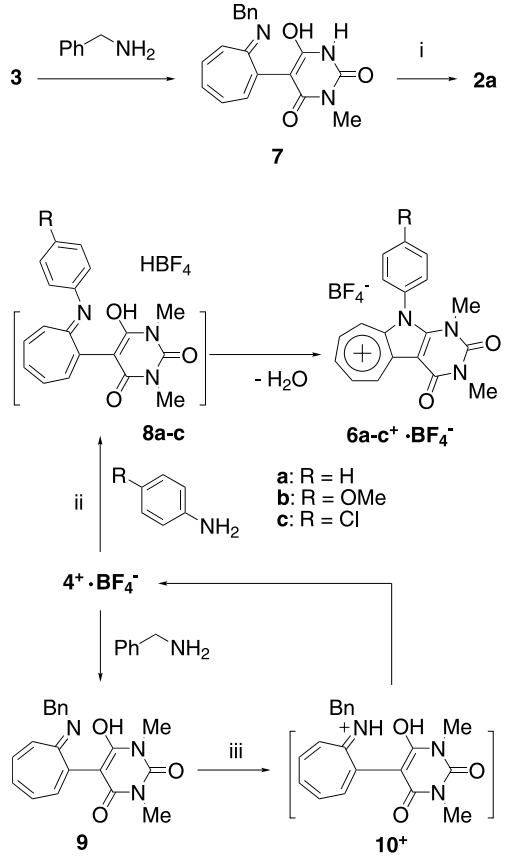

Scheme 1. Reagents and conditions: (i) 1,4-dioxane, reflux, 5 h; (ii) (a) CH_3CN, reflux, 3 h, (b) 42% aq HBF_4, Ac_2O, 0 °C, 1 h; (iii) 42% aq. HBF_4, Ac_2O, 0 °C, 1 h.

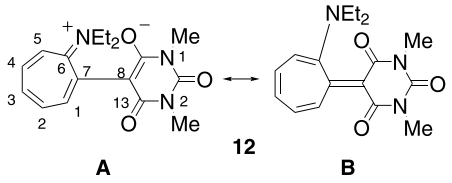

Figure 2. Numbering is shown according to the ORTEP drawing of **12**.

of isolated troponeimine intermediate **9** (Scheme 1) and N,N-disubstituted troponeimine **12** (Fig. 2) were investigated by inspection of their X-ray crystal analyses and spectral data including CV measurements. The remarkable structure of **12** having ionic C–O bonding between the imine-carbon atom and the oxygen atom of the barbituric acid moiety in the solid state was clarified. Thus, characteristics of **9** are rationalized by postulating sterically hindered and favorable conformation of the N-protonated troponeimine intermediates. Furthermore, the oxidizing ability of a series of $\mathbf{4}^+\cdot\mathbf{BF}_4^-$, $\mathbf{5}^+\cdot\mathbf{BF}_4^-$, $\mathbf{6a,e}^+\cdot\mathbf{BF}_4^-$ toward some amines was studied as well. Furthermore, mechanistic aspects of the amine-oxidation reaction are also postulated. We report herein the results in detail.

2. Results and discussion

2.1. Ring-transformation

As the ring transformation of **3a** to **2a**,**b**, we have reported that the thermal reaction of troponeimine **7**, obtained by the reaction of **3** with benzylamine, gives neutral pyrrole derivative **2a** (Scheme 1).[10] Thus, a reaction of $\mathbf{4}^+\cdot\mathbf{BF}_4^-$ with $PhNH_2$ was carried out to give the corresponding troponeimine **8a**, which is labile and easily cyclizes at room temperature to give $\mathbf{6a}^+$. Thus, a thermal reaction of $\mathbf{4}^+\cdot\mathbf{BF}_4^-$ with $PhNH_2$ was carried out to give $\mathbf{6a}^+\cdot\mathbf{BF}_4^-$ quantitatively (Scheme 1, Table 1, entry 1). In order to elucidate the generality of this method, reactions of $\mathbf{4}^+\cdot\mathbf{BF}_4^-$ with 4-substituted anilines were carried out (Table 1). The reactions of $\mathbf{4}^+\cdot\mathbf{BF}_4^-$ with 4-$MeOC_6H_4NH_2$ and 4-$ClC_6H_4NH_2$ afforded the corresponding $\mathbf{6b,c}^+\cdot\mathbf{BF}_4^-$ in quantitative yields, respectively (entries 2 and 3). On the reaction of $\mathbf{4}^+\cdot\mathbf{BF}_4^-$ with 4-$NCC_6H_4NH_2$, which has a strong electron-withdrawing substituent, addition reaction was not observed in the ^1H NMR monitoring during prolonged reaction time, and the starting materials were recovered quantitatively (cf. entry 4).

On the other hand, we have recently reported that the reaction of $\mathbf{4}^+\cdot\mathbf{BF}_4^-$ with benzylamine gives troponeimine **9** (Scheme 1).[12] While the reaction of **9** with HBF_4 regenerates $\mathbf{4}^+\cdot\mathbf{BF}_4^-$ (Scheme 1), thermal reaction of **9** resulted in the formation of a complicated mixture, and the expected compound $\mathbf{6d}^+\cdot\mathbf{BF}_4^-$ was not obtained.[12] Regarding the X-ray analysis of compounds $\mathbf{6a,e}^+\cdot\mathbf{BF}_4^-$, large steric hindrance between the N6-substituent and N7Me has been suggested.[14] Thus, the possible steric hindrance between the large benzyl group and the NMe group in **9** seems to inhibit the cyclization. Thus, in order to accomplish the ring-transformation of $\mathbf{4}^+\cdot\mathbf{BF}_4^-$ to $\mathbf{6d}^+\cdot\mathbf{BF}_4^-$, inhibition of the nucleophilic attack of oxygen of the barbituric acid moiety as well as acceleration of the

Table 1. Results for the reaction of $\mathbf{4}^{+}\cdot\mathbf{BF}_4^{-}$ with aniline and 4-substituted anilines

Entry	$\mathbf{4}^{+}\cdot\mathbf{BF}_4^{-}$	Aniline	Time[a]/h	Product	Yield[b]/%
1	$\mathbf{4}^{+}\cdot\mathbf{BF}_4^{-}$	$PhNH_2$	3	$\mathbf{6a}^{+}\cdot\mathbf{BF}_4^{-}$	100
2	$\mathbf{4}^{+}\cdot\mathbf{BF}_4^{-}$	$4\text{-}MeOC_6H_4NH_2$	3	$\mathbf{6b}^{+}\cdot\mathbf{BF}_4^{-}$	100
3	$\mathbf{4}^{+}\cdot\mathbf{BF}_4^{-}$	$4\text{-}ClC_6H_4NH_2$	3	$\mathbf{6c}^{+}\cdot\mathbf{BF}_4^{-}$	100
4	$\mathbf{4}^{+}\cdot\mathbf{BF}_4^{-}$	$4\text{-}NCC_6H_4NH_2$	24	None[c]	—

[a] Reaction was carried out in CH_3CN solution under reflux.
[b] Isolated yield.
[c] Reaction did not proceed and the starting materials were recovered quantitatively.

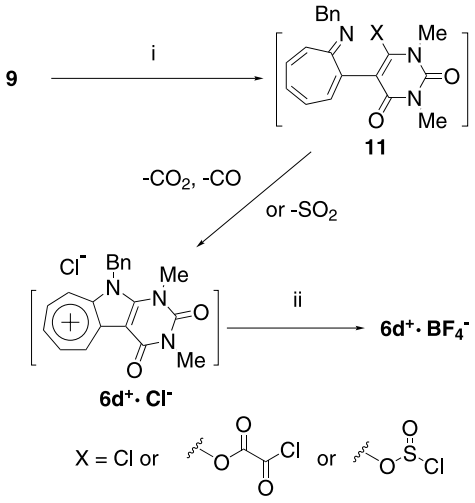

Scheme 2. Reagents and conditions: (i) $(COCl)_2$ or $SOCl_2$, conditions described in Table 2; (ii) 42% aq. HBF_4, Ac_2O, 0 °C, 1 h.

nucleophilic attack of nitrogen of the troponeimine moiety is necessary (vide infra). Thus, upon treatment with $(COCl)_2$ and $SOCl_2$, the hydroxyl group of **9** was expected to convert to a leaving group X, which can not attack the troponeimine moiety (Scheme 2). Under both conditions, the reaction of **9** with $(COCl)_2$ afforded a mixture of $\mathbf{6d}^{+}\cdot\mathbf{BF}_4^{-}$ and $\mathbf{4}^{+}\cdot\mathbf{BF}_4^{-}$ (Table 2, entries 1–3). In contrast, the reaction of **9** with $SOCl_2$ proceeded at room temperature to give $\mathbf{6d}^{+}\cdot\mathbf{BF}_4^{-}$ quantitatively (Table 2, entry 4).

Compound $\mathbf{6a}^{+}\cdot\mathbf{BF}_4^{-}$ was identified on the basis of a comparison of the physical data with those of the authentic specimen.[14] In addition, new compounds $\mathbf{6b–d}^{+}\cdot\mathbf{BF}_4^{-}$ were fully characterized on the basis of the ^1H and ^{13}C NMR, IR, and mass spectral data as well as elemental analysis. Furthermore, the CV measurement of $\mathbf{6b–d}^{+}\cdot\mathbf{BF}_4^{-}$ in CH_3CN exhibited irreversible reduction waves ($E1_{red}$), which are summarized in Table 3, together with those of the reference compounds. The irreversible nature is probably due to the formation of a radical species and its dimerization, as reported to be a typical property of uracil-annulated heteroazulenylium ions $\mathbf{4}^{+}\cdot\mathbf{BF}_4^{-}$,[12] $\mathbf{5}^{+}\cdot\mathbf{BF}_4^{-}$,[13] and $\mathbf{6a,e}^{+}\cdot\mathbf{BF}_4^{-}$.[14] While the $E1_{red}$ of $\mathbf{6d}^{+}\cdot\mathbf{BF}_4^{-}$ is similar to that of $\mathbf{6a}^{+}\cdot\mathbf{BF}_4^{-}$ (−0.84 V),[14] the $E1_{red}$ of $\mathbf{6b,c}^{+}\cdot\mathbf{BF}_4^{-}$ are less negative than that of $\mathbf{6a}^{+}\cdot\mathbf{BF}_4^{-}$. This feature is rationalized on the basis of the electron-withdrawing property of MeO- and Cl-substituted phenyl groups in $\mathbf{6b,c}^{+}\cdot\mathbf{BF}_4^{-}$, in which the substituted phenyl groups experience steric hindrance with the N7Me group and would twist against the plane of the heteroazulene unit.

2.2. Structural properties of troponeimines

We have recently reported that the reaction of $\mathbf{4}^{+}\cdot\mathbf{BF}_4^{-}$ with diethylamine gives the troponeimine **12** (Fig. 2).[12] Thus, the detailed characteristics of **9** and **12** are interesting

Table 2. Results for the reaction of imine **9** with $(COCl)_2$ and $SOCl_2$

Run	Additive	Solvent	Conditions	Product (yield[a]/%)
1	$(COCl)_2$	$(CH_2Cl)_2$	Room temperature, 1 h	$\mathbf{6d}^{+}\cdot\mathbf{BF}_4^{-}$ (26), $\mathbf{4}^{+}\cdot\mathbf{BF}_4^{-}$ (74)[b]
2	$(COCl)_2$	$(CH_2Cl)_2$	70 °C, 1 h	$\mathbf{6d}^{+}\cdot\mathbf{BF}_4^{-}$ (25), $\mathbf{4}^{+}\cdot\mathbf{BF}_4^{-}$ (75)[b]
3	$(COCl)_2$	None	Reflux, 3 h	$\mathbf{6d}^{+}\cdot\mathbf{BF}_4^{-}$ (78), $\mathbf{4}^{+}\cdot\mathbf{BF}_4^{-}$ (22)[b]
4	$SOCl_2$	None	Room temperature, 10 min	$\mathbf{6d}^{+}\cdot\mathbf{BF}_4^{-}$ (100)

[a] Isolated yield.
[b] Product ratio was calculated by ^1H NMR spectroscopy.

Table 3. Redox potentials of $\mathbf{6b–d}^{+}\cdot\mathbf{BF}_4^{-}$, **9**, and **12** and reference compounds $\mathbf{4}^{+}\cdot\mathbf{BF}_4^{-}$, $\mathbf{5}^{+}\cdot\mathbf{BF}_4^{-}$, and $\mathbf{6a,e}^{+}\cdot\mathbf{BF}_4^{-}$

Compound	Redox potential[a]		Compound	Redox potential[a]	
	$E1_{red}$	$E1_{ox}$		$E1_{red}$	$E1_{ox}$
$\mathbf{4}^{+}\cdot\mathbf{BF}_4^{-}$[b]	−0.58	—	$\mathbf{6d}^{+}\cdot\mathbf{BF}_4^{-}$	−0.84	—
$\mathbf{5}^{+}\cdot\mathbf{BF}_4^{-}$[b]	−0.53	—	$\mathbf{6e}^{+}\cdot\mathbf{BF}_4^{-}$[c]	−0.87	—
$\mathbf{6a}^{+}\cdot\mathbf{BF}_4^{-}$[d]	−0.84	—			
$\mathbf{6b}^{+}\cdot\mathbf{BF}_4^{-}$	−0.80	—	**9**	−1.40	+0.63
$\mathbf{6c}^{+}\cdot\mathbf{BF}_4^{-}$	−0.76	—	**12**	−1.85	+0.41

[a] V vs. $Ag/AgNO_3$; cathodic and anodic peak potentials.
[b] Ref. 10.
[c] Ref. 15.
[d] Ref. 13.

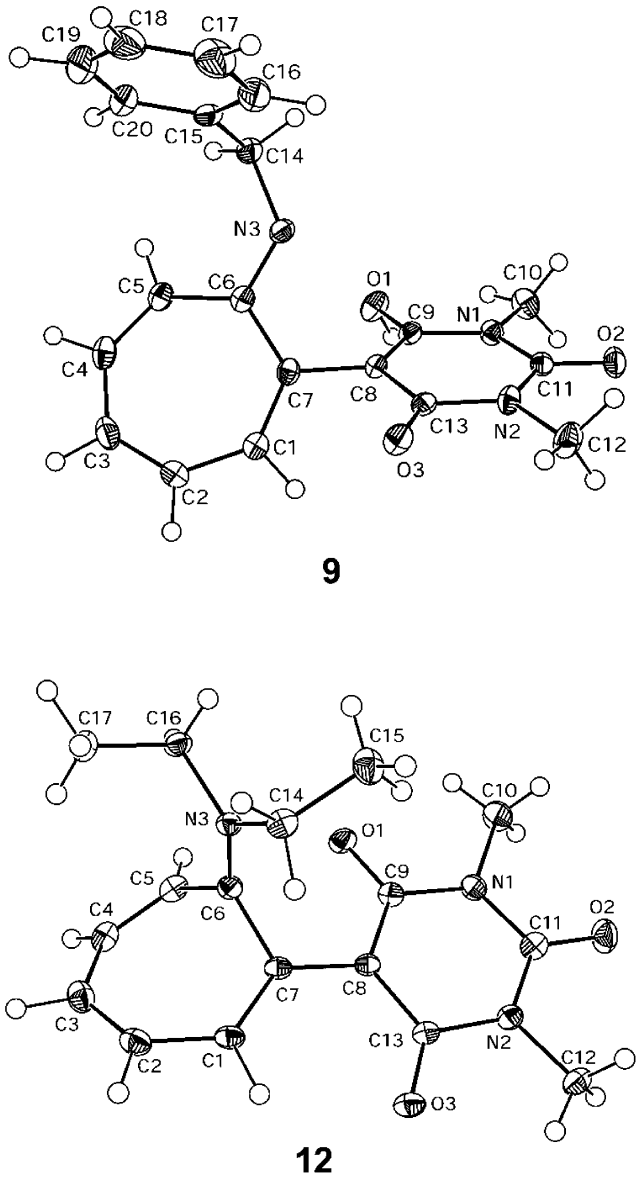

Figure 3. ORTEP drawing of **9** and **12** with thermal ellipsoid plot (50% probability).

in the view of clarifying the unreactive nature of **9** in the present ring transformation. Single crystals of **9** and **12** were obtained by recrystallization from $CHCl_3$ and AcOEt, respectively, and their ORTEP drawings are shown in Figure 3. The barbituric acid moiety of **9** has a nearly planar structure, while the troponeimine moiety has a boat shape, but the deformation from planarity is small. Furthermore, the troponeimine moiety of **9** shows a large bond alternation. In addition, the atomic distances of O1–C6 and N3–C9 are 3.039 and 3.023 Å, respectively (Table 4), and the dihedral angle of C6–C7–C8–C9 is 57.3°. On the other hand, the troponeimine moiety of **12** shows a large bond alternation as shown in the canonical structure **12-A** (Fig. 2, Table 4), which is supported by the ^1H and ^{13}C NMR study.[12] While the barbituric acid moiety of **12** has a nearly planar structure, the troponeimine moiety is highly distorted to a boat shape. A remarkable feature is the short atomic distance of O1–C6 (2.362 Å), which is larger than a typical O–C covalent bond (1.43 Å),[16] but it is considerably shorter than the sum of the van der Waals radii (3.25 Å).[16] This is probably due to the interaction between the O1 and the C6; however, the sum of the bond angles of N3–C6–C5, N3–C6–C7, and C5–C6–C7 is 359.1°, and thus, the C6 carbon atom exists as sp^2 hybridization. Furthermore, the short bond length of the N3–C6 (1.304 Å) suggests its double bond character, and the bond length of the O1–C9 is similar to that of the O3–C13. These features support that the interaction of the O1–C6 is an ionic bonding, and not a covalent bonding in the solid state. The remarkable structure of **12** seems close to the transition state of the intramolecular nucleophilic addition of the O1 atom reverting to the furan-ring of $\mathbf{4}^+$: intermediate $\mathbf{10}^+$, generated by protonation of **9**, may have a structure similar to that of **12**, and thus, the acidic reaction of **9** using aq. HBF_4 easily regenerate $\mathbf{4}^+\cdot\mathbf{BF}_4^-$ (Scheme 1). Thus, in order to accomplish the ring transformation of $\mathbf{4}^+\cdot\mathbf{BF}_4^-$ to $\mathbf{6d}^+\cdot\mathbf{BF}_4^-$, $(COCl)_2$ or $SOCl_2$ is required for cyclization of **9** to $\mathbf{6d}^+\cdot\mathbf{BF}_4^-$ (vide supra).

On the other hand, in the ^1H NMR spectrum of **12**, the signals of N1Me and N3Me appear equivalent (δ 3.34) at room temperature.[12] They appear as two sharp singlets at low temperature (−90 °C), while the signals of the seven-membered ring show no appreciable change. Thus, rapid rotation around the C7–C8 bond of **12** (Fig. 2) clearly occurs on the NMR time scale at room temperature in solution. Through variable temperature ^1H NMR measurement of **12**, the coalescence temperature was determined to be 261 K, and the chemical shift difference between N1Me and N3Me was 50.6 Hz. Consequently, rotational barrier ($\Delta G^{\ddagger}$) around the C7–C8 bond was determined to be 12.75 kcal mol^{-1}. In the ^{13}C NMR spectrum of **12** at −90 °C, the signals of two carbonyl-carbons C9 and C13 appear as two sharp signals (δ_C 160.3 and 161.5), which is not changed from the

Table 4. Bond lengths and atomic distance of **9** and **12** obtained by X-ray structure analysis

Bond[a]	Bond length/Å		Bond[a]	Bond length/Å	
	9	**12**		**9**	**12**
O1–C6[b]	3.039(3)	2.362(3)	C1–C7	1.372(4)	1.375(3)
N3–C9[b]	3.023(3)	3.300(3)	N3–C6	1.331(4)	1.305(3)
C1–C2	1.429(4)	1.444(3)	C7–C8	1.479(4)	1.448(3)
C2–C3	1.348(4)	1.369(4)	C8–C9	1.408(4)	1.414(3)
C3–C4	1.419(4)	1.429(4)	C8–C13	1.421(4)	1.425(3)
C4–C5	1.354(4)	1.359(4)	O1–C9	1.242(3)	1.243(3)
C5–C6	1.436(3)	1.457(3)	O3–C13	1.243(3)	1.239(3)
C6–C7	1.459(4)	1.486(3)			

[a] The numbering is shown in Figure 3.
[b] Atomic distance.

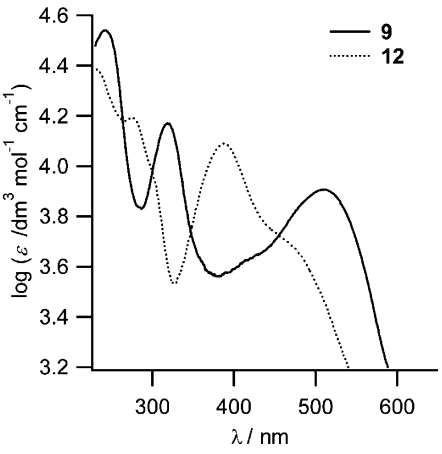

Figure 4. UV–vis spectra of **9** and **12** in CH_3CN.

equivalent signal at room temperature (δ_C 162.1).[12] In addition, the chemical shift of the iminium-carbon C6 at −90 °C (δ_C 172.6) is similar to the corresponding signal at room temperature (δ_C 174.4),[12] thus, the interaction between the carbonyl oxygen atom O1 and the C6 would not be large in solution.

The UV–vis spectral data of **9** and **12** in CH_3CN are summarized in Figure 4. The spectra of **9** and **12** show remarkable difference, and the longest wavelength absorption maximum of **12** shows a blue-shift by 122 nm, as compared with that of **9**. Furthermore, the reduction and oxidation potentials of **9** and **12** in CH_3CN were determined by cyclic voltammetry (CV), and each reduction wave and oxidation wave are irreversible. While the reduction potentials ($E1_{red}$) of **9** and **12** are −1.40 and −1.85 V, respectively, their oxidation potentials ($E1_{ox}$) are +0.63 and +0.41 V, respectively. Thus, the values ($E1_{red}$ and $E1_{ox}$) of **12** are more negative than those of **9**. After the first cycle of CV measurement of **12**, another reversible reduction wave was recorded at +0.10 V, which is probably the reduction wave of **14**, generated by cyclization of **13** under CV measurement (Scheme 3). After generation of **14** and subsequent measurement in the limited range of −0.20 and +0.40 V, decay of this wave was observed due to the slow ring-opening reaction of **15** giving **12**. In contrast, neutral imine **9** does not exhibit behavior similar to that of **12**.

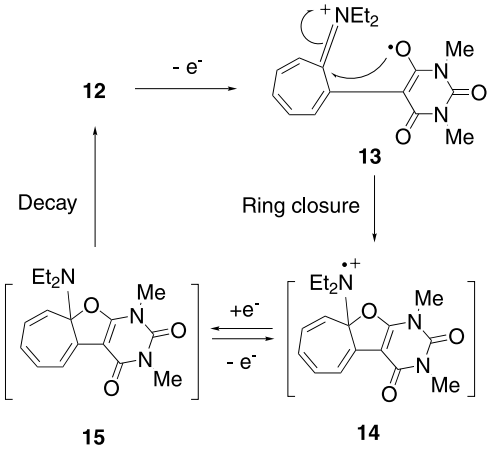

Scheme 3.

2.3. Autorecycling oxidation

We have previously reported that compounds $\mathbf{4}^+\cdot\mathbf{BF}_4^-$, $\mathbf{5}^+\cdot\mathbf{BF}_4^-$, and $\mathbf{6a,e}^+\cdot\mathbf{BF}_4^-$ undergo autorecycling oxidation of some alcohols to give the corresponding carbonyl compounds under photo-irradiation.[12–14] In this context and in a search for other functions, we examined the oxidation of some amines by using $\mathbf{4}^+\cdot\mathbf{BF}_4^-$ and $\mathbf{6a,e}^+\cdot\mathbf{BF}_4^-$ as well as sulfur analogue $\mathbf{5}^+\cdot\mathbf{BF}_4^-$ under aerobic and photo-irradiation conditions (RPR-100, 350 nm lamps). We found that a series of compounds $\mathbf{4}^+\cdot\mathbf{BF}_4^-$, $\mathbf{5}^+\cdot\mathbf{BF}_4^-$, and $\mathbf{6a,e}^+\cdot\mathbf{BF}_4^-$ have an oxidizing ability toward some amines to give the corresponding imines. Imines **20** are produced at first; and they react with other amines to result in the formation of $R^1R^2C{=}N{-}CHR^1R^2$ (**21**) (Scheme 4). The results are summarized in Table 5. Direct irradiation of the amines in the absence of $\mathbf{4}^+\cdot\mathbf{BF}_4^-$, $\mathbf{5}^+\cdot\mathbf{BF}_4^-$, and $\mathbf{6a,e}^+\cdot\mathbf{BF}_4^-$ (named 'blank') gives the imines in low to modest yields. Thus, the yields of imines are calculated by subtraction of the 'blank' yield from the yields obtained in the presence of $\mathbf{4}^+\cdot\mathbf{BF}_4^-$, $\mathbf{5}^+\cdot\mathbf{BF}_4^-$, and $\mathbf{6a,e}^+\cdot\mathbf{BF}_4^-$. More than 100% yields are obtained [based on compounds $\mathbf{4}^+\cdot\mathbf{BF}_4^-$, $\mathbf{5}^+\cdot\mathbf{BF}_4^-$, and $\mathbf{6a,e}^+\cdot\mathbf{BF}_4^-$] (Table 5), and thus, autorecycling oxidation clearly proceeds; however, cyclohexylamine was not oxidized (Table 5, entries 26–29). In order to clarify the details of the oxidizing reaction, time dependency of the yields of the imines was investigated as summarized in Table 5 (entries 1–16) and Figure 5. Concerning the oxidizing reaction using $\mathbf{4}^+\cdot\mathbf{BF}_4^-$, the yield of benzaldimine was increased simply as the irradiation time was prolonged to 8 h. After irradiation for 12 and 16 h, the yield of benzaldimine is not so increased, suggesting plausible decomposition of $\mathbf{4}^+\cdot\mathbf{BF}_4^-$. A Similar feature is observed in the oxidizing reaction by using $\mathbf{5}^+\cdot\mathbf{BF}_4^-$, and $\mathbf{6a,e}^+\cdot\mathbf{BF}_4^-$. The photo-irradiation of CD_3CN solution of $\mathbf{4}^+\cdot\mathbf{BF}_4^-$, $\mathbf{5}^+\cdot\mathbf{BF}_4^-$, and $\mathbf{6a,e}^+\cdot\mathbf{BF}_4^-$ in the absence of amine under aerobic conditions, decomposition of $\mathbf{4}^+\cdot\mathbf{BF}_4^-$, $\mathbf{5}^+\cdot\mathbf{BF}_4^-$, and $\mathbf{6a,e}^+\cdot\mathbf{BF}_4^-$ was not observed as monitored by their ^1H NMR spectra. Thus, the decomposition of $\mathbf{4}^+\cdot\mathbf{BF}_4^-$, $\mathbf{5}^+\cdot\mathbf{BF}_4^-$, and $\mathbf{6a,e}^+\cdot\mathbf{BF}_4^-$ would occur in their oxidation cycle.

Furthermore, in the oxidation of benzylamine by using $\mathbf{5}^+\cdot\mathbf{BF}_4^-$, and $\mathbf{6a,e}^+\cdot\mathbf{BF}_4^-$, the yield of the imine became higher in the order $\mathbf{6e}^+\cdot\mathbf{BF}_4^- < \mathbf{6a}^+\cdot\mathbf{BF}_4^- < \mathbf{5}^+\cdot\mathbf{BF}_4^-$ (Table 5, entries 5–16). This fact is probably ascribed to the $E1_{red}$ values in the order $\mathbf{6e}^+\cdot\mathbf{BF}_4^-$ (−0.87 V)[14] > $\mathbf{6a}^+\cdot\mathbf{BF}_4^-$ (−0.84 V)[14] > $\mathbf{5}^+\cdot\mathbf{BF}_4^-$ (−0.53 V).[13] [The reduction potentials of $\mathbf{5}^+\cdot\mathbf{BF}_4^-$, and $\mathbf{6a,e}^+\cdot\mathbf{BF}_4^-$ in the ground state would be correlated with their LUMO's, and thus, the LUMO's of these compounds would be lower in the order $\mathbf{6e}^+\cdot\mathbf{BF}_4^- > \mathbf{6a}^+\cdot\mathbf{BF}_4^- > \mathbf{5}^+\cdot\mathbf{BF}_4^-$. In the excited state of these compounds, the electron-accepting orbital would be the singly occupied HOMO's. In as much as the UV–vis spectra of these compounds are similar, and thus, the energy level of HOMO's of the compounds is expected to be lower in the order $\mathbf{6e}^+\cdot\mathbf{BF}_4^- > \mathbf{6a}^+\cdot\mathbf{BF}_4^- > \mathbf{5}^+\cdot\mathbf{BF}_4^-$.] A similar tendency was observed in the cases of the oxidation of 1-phenylethylamine and hexylamine (Table 5, entries 19–21 and 23–25). Benzylamine and hexylamine are oxidized more effectively by using $\mathbf{4}^+\cdot\mathbf{BF}_4^-$ (Table 5, entries 4 and 22), which has a lower

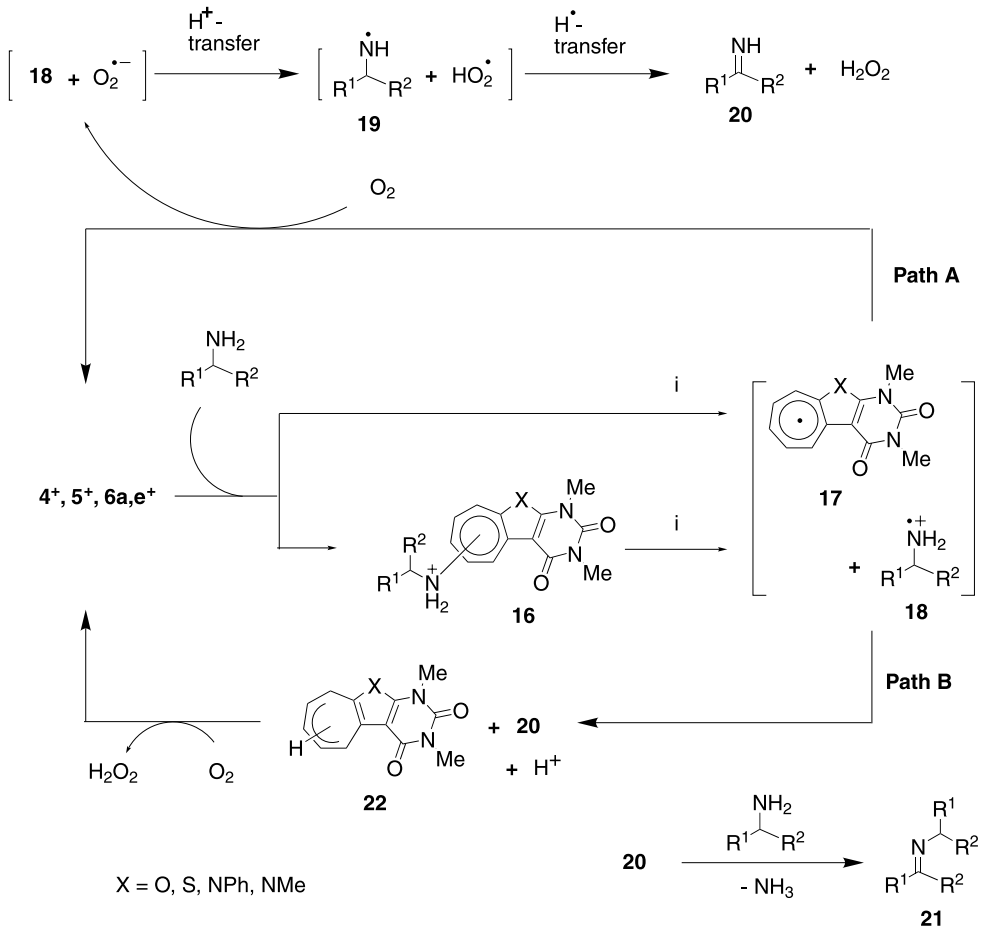

Scheme 4. Reagents and conditions: (i) hν, aerobic, CH_3CN, room temperature.

oxidizing ability toward 1-phenylethylamine as compared to $\mathbf{5}^+\cdot\mathbf{BF}_4^-$ (cf. entries 18 and 19). The feature is probably due to the ring-opening reaction of $\mathbf{4}^+\cdot\mathbf{BF}_4^-$ with some amines. However, in the oxidation of benzylamine by using isolated **9**, the yield of the imine (643%) is lower than that by using $\mathbf{4}^+\cdot\mathbf{BF}_4^-$ (8161%) (Table 5, entries 17 and 4). Thus, the presence of HBF_4 is necessary for the effective oxidizing cycle, suggesting that the reaction of **9** with HBF_4 would regenerate $\mathbf{4}^+\cdot\mathbf{BF}_4^-$ in the oxidizing cycle.

In a search for the substituent effect of benzylamine toward oxidation, the oxidation reactions of 4-substituted

Table 5. Autorecycling oxidation of some amines by $\mathbf{4}^+\cdot\mathbf{BF}_4^-$–$\mathbf{6a,e}^+\cdot\mathbf{BF}_4^-$ under photo-irradiation[a]

Entry	Compound	Amine	Time/h	Yield[b]/%	Entry	Compound	Amine	Time/h	Yield[b]/%
1	$\mathbf{4}^+\cdot\mathbf{BF}_4^-$	$PhCH_2NH_2$	4	4601	18	$\mathbf{4}^+\cdot\mathbf{BF}_4^-$	$PhCH(Me)NH_2$	16	3947
2	$\mathbf{4}^+\cdot\mathbf{BF}_4^-$	$PhCH_2NH_2$	8	7559	19	$\mathbf{5}^+\cdot\mathbf{BF}_4^-$	$PhCH(Me)NH_2$	16	7040
3	$\mathbf{4}^+\cdot\mathbf{BF}_4^-$	$PhCH_2NH_2$	12	7951	20	$\mathbf{6a}^+\cdot\mathbf{BF}_4^-$	$PhCH(Me)NH_2$	16	3533
4	$\mathbf{4}^+\cdot\mathbf{BF}_4^-$	$PhCH_2NH_2$	16	8161	21	$\mathbf{6e}^+\cdot\mathbf{BF}_4^-$	$PhCH(Me)NH_2$	16	2367
5	$\mathbf{5}^+\cdot\mathbf{BF}_4^-$	$PhCH_2NH_2$	4	3552	22	$\mathbf{4}^+\cdot\mathbf{BF}_4^-$	Hexylamine	16	7464
6	$\mathbf{5}^+\cdot\mathbf{BF}_4^-$	$PhCH_2NH_2$	8	5076	23	$\mathbf{5}^+\cdot\mathbf{BF}_4^-$	Hexylamine	16	4457
7	$\mathbf{5}^+\cdot\mathbf{BF}_4^-$	$PhCH_2NH_2$	12	6846	24	$\mathbf{6a}^+\cdot\mathbf{BF}_4^-$	Hexylamine	16	2557
8	$\mathbf{5}^+\cdot\mathbf{BF}_4^-$	$PhCH_2NH_2$	16	6993	25	$\mathbf{6e}^+\cdot\mathbf{BF}_4^-$	Hexylamine	16	1564
9	$\mathbf{6a}^+\cdot\mathbf{BF}_4^-$	$PhCH_2NH_2$	4	1476	26	$\mathbf{4}^+\cdot\mathbf{BF}_4^-$	Cyclohexylamine	16	0[c]
10	$\mathbf{6a}^+\cdot\mathbf{BF}_4^-$	$PhCH_2NH_2$	8	2552	27	$\mathbf{5}^+\cdot\mathbf{BF}_4^-$	Cyclohexylamine	16	0[c]
11	$\mathbf{6a}^+\cdot\mathbf{BF}_4^-$	$PhCH_2NH_2$	12	4133	28	$\mathbf{6a}^+\cdot\mathbf{BF}_4^-$	Cyclohexylamine	16	0[c]
12	$\mathbf{6a}^+\cdot\mathbf{BF}_4^-$	$PhCH_2NH_2$	16	4175	29	$\mathbf{6e}^+\cdot\mathbf{BF}_4^-$	Cyclohexylamine	16	0[c]
13	$\mathbf{6e}^+\cdot\mathbf{BF}_4^-$	$PhCH_2NH_2$	4	455	30	$\mathbf{4}^+\cdot\mathbf{BF}_4^-$	$4\text{-}MeOC_6H_4CH_2NH_2$	16	6278
14	$\mathbf{6e}^+\cdot\mathbf{BF}_4^-$	$PhCH_2NH_2$	8	1385	31	$\mathbf{4}^+\cdot\mathbf{BF}_4^-$	$4\text{-}MeC_6H_4CH_2NH_2$	16	7967
15	$\mathbf{6e}^+\cdot\mathbf{BF}_4^-$	$PhCH_2NH_2$	12	2993	32	$\mathbf{4}^+\cdot\mathbf{BF}_4^-$	$4\text{-}ClC_6H_4CH_2NH_2$	16	8362
16	$\mathbf{6e}^+\cdot\mathbf{BF}_4^-$	$PhCH_2NH_2$	16	3000	33	$\mathbf{4}^+\cdot\mathbf{BF}_4^-$	$4\text{-}PyCH_2NH_2$	16	6789
17	**9**	$PhCH_2NH_2$	16	643					

Isolated by converting to the corresponding 2,4-dinitrophenylhydrazone.

[a] CH_3CN solution was irradiated by RPR-100, 350 nm lamps under aerobic conditions.

[b] Based on $\mathbf{4}^+\cdot\mathbf{BF}_4^-$, $\mathbf{5}^+\cdot\mathbf{BF}_4^-$, and $\mathbf{6a,e}^+\cdot\mathbf{BF}_4^-$ used; the yield is calculated by subtraction of the 'blank' yield from the total yield of carbonyl compound in the presence of $\mathbf{4}^+\cdot\mathbf{BF}_4^-$, $\mathbf{5}^+\cdot\mathbf{BF}_4^-$, and $\mathbf{6a,e}^+\cdot\mathbf{BF}_4^-$.

[c] The blank yield was higher than the yield in the presence of $\mathbf{4}^+\cdot\mathbf{BF}_4^-$, $\mathbf{5}^+\cdot\mathbf{BF}_4^-$, and $\mathbf{6a,e}^+\cdot\mathbf{BF}_4^-$.

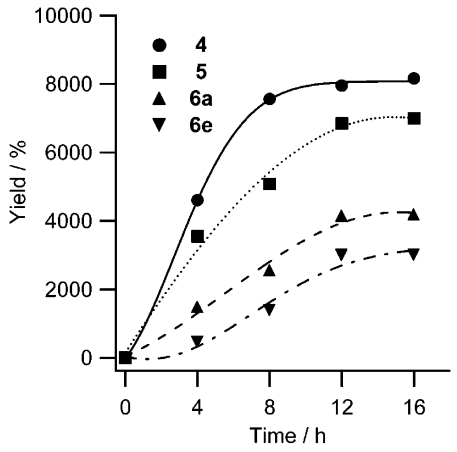

Figure 5. Time dependency of autorecycling oxidation of benzylamine by using $\mathbf{4}^{+}\cdot\mathbf{BF}_4^{-}$, $\mathbf{5}^{+}\cdot\mathbf{BF}_4^{-}$, and $\mathbf{6a,e}^{+}\cdot\mathbf{BF}_4^{-}$.

benzylamines and picolylamine were carried out by using $\mathbf{4}^{+}\cdot\mathbf{BF}_4^{-}$ under aerobic and photo-irradiation conditions (Table 5, entries 30–33). The yields of imines are plotted against the Hammet constants σ_p[17] of the substituents on the phenyl group and 4-picolylamine in Figure 6. The plots seem to show a maximum value, and the yield of photo-induced oxidation of the benzylamines becomes low at either the high value (σ_p 0.23, 4-$ClC_6H_4CH_2NH_2$) or the low value (σ_p −0.27, 4-$MeOC_6H_4CH_2NH_2$). The yields of the imine derived from 4-picolylamine, which corresponds to the benzylamine having a strong electron-withdrawing substituent, becomes low and may be close to the yield expected from 4-nitrobenzylamine. Thus, the oxidizing reaction by using $\mathbf{4}^{+}\cdot\mathbf{BF}_4^{-}$ becomes less effective for the amines, which have both lower and higher oxidation potential. This feature is similar to the cases of the photo-induced oxidizing reaction of benzy alcohol by using a flavin analogue[18] and the case of photo-induced oxidizing reaction of benzylamine by using **2a**,**b**,[10] and thus, it is rationalized by the pathways via a tropyl radical intermediate (vide infra).

The mechanistic pathways for the present oxidation of amines are depicted in Scheme 4 by using general structures.[18] The electron-transfer from amine to the excited state of $\mathbf{4}^{+}$, $\mathbf{5}^{+}$, and $\mathbf{6a,b}^{+}$ would occur to produce radicals **17** and a cation radical **18**. On the other hand, the amine-adducts obtained by the reaction of $\mathbf{4}^{+}$, $\mathbf{5}^{+}$, and $\mathbf{6a,e}^{+}\cdot\mathbf{BF}_4^{-}$ with amines, are stable in solution in the dark.[12–14] Thus, there is also a possibility that the homolysis of **16** by photo irradiation would afford **17** and **18** directly. An electron transfer from radical species **17** to a molecular oxygen would regenerate $\mathbf{4}^{+}$, $\mathbf{5}^{+}$, and $\mathbf{6a,e}^{+}$, and the superoxide anion radical, since tropyl radical derivatives are known to be readily oxidized by molecular oxygen.[19] Then, a proton-transfer from cation radical **18** to a superoxide anion radical occurs to result in the formation of the products **20** and H_2O_2 (Path A). Compound **20** reacts with excess amine to give imine **21**. Substituted benzylamine having a more negative oxidation potential seems to favor the electron transfer process from amine to the excited state of $\mathbf{4}^{+}$, $\mathbf{5}^{+}$, and $\mathbf{6a,e}^{+}$, but disfavors the proton transfer process from the cation radical **18** to the superoxide anion radical. On the contrary, substituted benzylamine having a more positive oxidation potential disfavors the electron transfer process from amine to the excited state of $\mathbf{4}^{+}$, $\mathbf{5}^{+}$, and $\mathbf{6a,e}^{+}$, while the proton transfer process from cation radical **18** to the superoxide anion radical becomes more favorable. As such, a sensitive balance between the electron donor ability of amine and the proton donor ability of cation radical **18** is required to achieve the efficient photo-induced oxidation reaction of amines. There may be an alternative mechanistic pathway (Path B), in which compound **22** and the imine **20** are generated directly from **17** and **18**; the former compound is oxidized under aerobic and photo-irradiation conditions to regenerate $\mathbf{4}^{+}$, $\mathbf{5}^{+}$, and $\mathbf{6a,e}^{+}$. Under aerobic and photo-irradiation conditions, the CD_3CN solution of **22** was easily oxidized to regenerate $\mathbf{4}^{+}$, $\mathbf{5}^{+}$, and $\mathbf{6a,e}^{+}$ quantitatively. Thus, autorecycling oxidation would also be possible in this Path B. However, attempted detection of compound **17** or its dimers or compound **22** was unsuccessful in the oxidation reaction of benzylamine under degassed and photo-irradiation conditions (degassed by freeze–pump–thaw cycles). Thus, we prefer the former pathway (Path A).

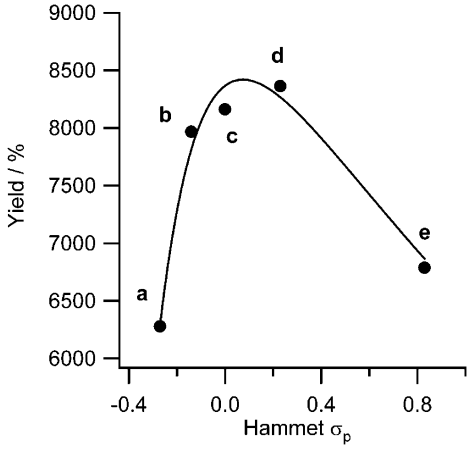

Figure 6. The Hammet plot of autorecycling oxidation of 4-substituted benzylamine by $\mathbf{4}^{+}\cdot\mathbf{BF}_4^{-}$. (a: 4-$MeOC_6H_4CH_2NH_2$, b: 4-$MeC_6H_4CH_2NH_2$, c: $PhCH_2NH_2$, d: 4-$ClC_6H_4CH_2NH_2$, e: 4-$PyCH_2NH_2$).

3. Conclusion

The ring transformation of $\mathbf{4}^{+}\cdot\mathbf{BF}_4^{-}$ to the corresponding pyrrole derivatives $\mathbf{6a–d}^{+}\cdot\mathbf{BF}_4^{-}$ was accomplished. Furthermore, the detailed characteristics of troponeimine intermediates **9** and **12** were clarified by the inspection of their X-ray crystal analyses, NMR, UV–vis spectra, and CV measurements. Novel photo-induced oxidation reaction of $\mathbf{4}^{+}\cdot\mathbf{BF}_4^{-}$, $\mathbf{5}^{+}\cdot\mathbf{BF}_4^{-}$, and $\mathbf{6a,e}^{+}\cdot\mathbf{BF}_4^{-}$ toward some amines under aerobic conditions was clarified to give the corresponding imines in more than 100% yield [based on compounds $\mathbf{4}^{+}$, $\mathbf{5}^{+}$, and $\mathbf{6a,e}^{+}$], suggesting the oxidation reaction occurs in an autorecycling process. Mechanistic aspects of the amine-oxidation are also postulated.

4. Experimental

4.1. General

IR spectra were recorded on a HORIBA FT-710

spectrometer. Mass spectra and high-resolution mass spectra were run on JMS-AUTOMASS 150 and JMS-SX102A spectrometers. Unless otherwise specified, ^{1}H and ^{13}C NMR spectra were recorded on JNM-lambda500 and AVANCE600 spectrometers using CD_3CN as a solvent, and the chemical shifts are given relative to internal $SiMe_4$ standard; *J*-values are given in Hz. Mps were recorded on a Yamato MP-21 apparatus and were uncorrected.

4.2. Ring transformation of $4^+ \cdot BF_4^-$ to $6a–c^+ \cdot BF_4^-$

To a solution of $\mathbf{4}^+ \cdot \mathbf{BF_4^-}$ (99 mg, 0.3 mmol) in CH_3CN (10 mL) was added aniline or 4-substituted aniline (1.2 mmol), and the mixture was heated under reflux until the reaction was completed (Table 1). The mixture was concentrate in vacuo, the resulting residue was dissolved in a mixture of acetic anhydride (5 mL) and 42% aq HBF_4 (1 mL) at 0 °C, and it was stirred for another 1 h. To the mixture was added Et_2O (50 mL) and the precipitates were collected by filtration to give products $\mathbf{6a–c}^+ \cdot \mathbf{BF_4^-}$ (Table 1). Compound $\mathbf{6a}^+ \cdot \mathbf{BF_4^-}$ was identical with the authentic specimen.[14]

4.2.1. 7,9-Dimethyl-6-(4′-methoxyphenyl)cyclohepta[*b*]-pyrimido[5,4-*d*]pyrrole-8(7*H*), 10(9*H*)-dionylium tetrafluoroborate ($\mathbf{6b}^+ \cdot \mathbf{BF_4^-}$). Orange prisms; mp 227–230 °C dec (from CH_3CN/Et_2O); ^{1}H NMR (500 MHz, CD_3CN) δ 3.17 (3H, s, 7-Me), 3.46 (3H, s, 9-Me), 3.95 3H, s, OMe), 7.27 (2H, d, J=9.0 Hz, Ph-3′, 5′), 7.59 (2H, d, J=9.0 Hz, Ph-2′, 6′), 8.31 (1H, d, J=10.2 Hz, H-5), 8.37 (1H, dd, J=10.2, 9.7 Hz, H-4), 8.56 (1H, dd, J=9.7, 9.5 Hz, H-3), 8.63 (1H, dd, J=10.3, 9.5 Hz, H-2), 9.94 (1H, d, J=10.3 Hz, H-1); ^{13}C NMR (150.9 MHz, CD_3CN) δ 29.1, 33.5, 56.9, 99.8, 116.9, 126.3, 131.8, 134.1, 139.8, 141.2, 143.4, 143.6, 145.8, 151.1, 152.2, 153.5, 159.0, 163.5; IR (KBr) ν 1717, 1675, 1084 cm^{-1}; MS (FAB) *m/z* 348 (M^+-BF_4); HRMS calcd for $C_{20}H_{18}BF_4N_3O_3$: 348.1347 ($M-BF_4$). Found: 348.1391 (M^+-BF_4). Anal. calcd for $C_{20}H_{18}BF_4N_3O_3$: C, 55.20; H, 4.17; N, 9.66. Found: C, 54.95; H, 4.08; N, 9.43.

4.2.2. 6-(4′-Chlorophenyl)-7,9-dimethylcyclohepta[*b*]-pyrimido[5,4-*d*]pyrrole-8(7*H*), 10(9*H*)-dionylium tetrafluoroborate ($\mathbf{6c}^+ \cdot \mathbf{BF_4^-}$). Greenish prisms; mp 266–269 °C dec (from CH_3CN/Et_2O); ^{1}H NMR (500 MHz, CD_3CN) δ 3.17 (3H, s, 7-Me), 3.46 (3H, s, 9-Me), 7.70 (2H, d, J=8.8 Hz, Ph-2′, 6′), 7.80 (2H, d, J=8.8 Hz, Ph-3′, 5′), 8.29 (1H, d, J=10.2 Hz, H-5), 8.37 (1H, dd, J=10.2, 9.8 Hz, H-4), 8.58 (1H, dd, J=9.8, 9.7 Hz, H-3), 8.65 (1H, dd, J=10.2, 9.7 Hz, H-2), 9.95 (1H, d, J=10.2 Hz, H-1); ^{13}C NMR (150.9 MHz, CD_3CN) δ 29.2, 33.8, 100.0, 132.1, 132.3, 133.1, 134.2, 139.2, 139.9, 141.4, 143.7, 143.9, 146.1, 150.6, 152.0, 153.4, 159.0; IR (KBr) ν 1722, 1675, 1084 cm^{-1}; MS (FAB) *m/z* 352 (M^+-BF_4); HRMS calcd for $C_{19}H_{15}BClF_4N_3O_2$: 352.0853 ($M-BF_4$). Found: 352.0858 (M^+-BF_4). Anal. calcd for $C_{19}H_{15}BClF_4N_3O_2$: C, 51.91; H, 3.44; N, 9.56. Found: C, 51.80; H, 3.38; N, 9.46.

4.3. Reaction of 9 with $(COCl)_2$ in $(CH_2CCl)_2$

To a solution of **9** (35 mg, 0.1 mmol) in $(CH_2Cl)_2$ (2 mL) was added $(COCl)_2$ (65 mg, 0.5 mmol), and the mixture was stirred at room temperature or 70 °C for 1 h. After the reaction was completed, the mixture was concentrated in vacuo. The resulting residue was dissolved in a mixture of acetic anhydride (1 mL) and 42% aq HBF_4 (0.2 mL) at 0 °C, and the mixture was stirred for another 1 h. To the mixture was added Et_2O (10 mL) and the precipitates were collected by filtration to give a mixture of $\mathbf{6d}^+ \cdot \mathbf{BF_4^-}$ and $\mathbf{4}^+ \cdot \mathbf{BF_4^-}$ (Table 2, runs 1 and 2).

4.4. Reaction of 9 with $(COCl)_2$ without solvent

A solution of **9** (35 mg, 0.1 mmol) in $(COCl)_2$ (2 mL) was heated under reflux for 3 h. After the reaction was completed, the mixture was concentrate in vacuo. The resulting residue was dissolved in a mixture of acetic anhydride (1 mL) and 42% aq HBF_4 (0.2 mL) at 0 °C, and the mixture was stirred for another 1 h. To the mixture was added Et_2O (10 mL) and the precipitates were collected by filtration to give a mixture of $\mathbf{6d}^+ \cdot \mathbf{BF_4^-}$ and $\mathbf{4}^+ \cdot \mathbf{BF_4^-}$ (Table 2, run 3).

4.5. Reaction of 9 with $SOCl_2$

A solution of **9** (35 mg, 0.1 mmol) in $SOCl_2$ (2 mL) was heated under reflux for 3 h. After the reaction was completed, the mixture was concentrate in vacuo. The resulting residue was dissolved in a mixture of acetic anhydride (1 mL) and 42% aq HBF_4 (0.2 mL) at 0 °C, and the mixture was stirred for another 1 h. To the mixture was added Et_2O (10 mL) and the precipitates were collected by filtration to give a single product $\mathbf{6d}^+ \cdot \mathbf{BF_4^-}$ (Table 2, run 5).

4.5.1. 7,9-Dimethyl-6-benzylcyclohepta[*b*]pyrimido [5,4-*d*]pyrrole-8(7*H*),10(9*H*)-dionylium tetrafluoroborate ($\mathbf{6d}^+ \cdot \mathbf{BF_4^-}$). Orange prisms; mp 210–211 °C (from CH_3CN/Et_2O); ^{1}H NMR (600 MHz, CD_3CN) δ 3.45 (3H, s, 9-Me), 3.75 (3H, s, 7-Me), 6.12 (2H, s, CH_2), 7.19–7.21 (2H, m, *m*-Ph), 7.40–7.44 (3H, m, *o*,*p*-Ph), 8.44 (1H, dd, J=10.2, 10.0 Hz, H-2), 8.57 (1H, dd, J=10.0, 9.5 Hz, H-4), 8.62 (1H, dd, J=10.2, 9.5 Hz, H-3), 8.76 (1H, d, J=10.2 Hz, H-5), 9.97 (1H, d, J=10.2 Hz, H-1); ^{13}C NMR (150.9 MHz, CD_3CN) δ 29.0, 33.8, 51.2, 100.5, 126.4, 129.6, 130.3, 133.0, 134.9, 139.6, 141.1, 143.6, 143.9, 145.8, 149.4, 152.1, 154.2, 158.8; IR (KBr) ν 1717, 1675, 1084 cm^{-1}; MS (FAB) *m/z* 332 (M^+-BF_4); HRMS calcd for $C_{20}H_{18}BF_4N_3O_2$: 332.1399 ($M-BF_4$). Found: 332.1379 (M^+-BF_4). Anal. calcd for $C_{20}H_{18}BF_4N_3O_2+1/5H_2O$: C, 56.82; H, 4.39; N, 9.94. Found: C, 56.75; H, 4.42; N, 9.96.

4.6. X-ray structure determination of 9[†]

Reddish plate, $C_{20}H_{19}N_3O_3+2CHCl_3$, M=588.14, monoclinic, space group $P2_1/c$, a=11.1393(4) Å, b=19.5525(8) Å, c=11.6973(6) Å, β=94.569(2) °, V=2539.6(2) Å^3, Z=4, D_c=1.538 g mL^{-1}, crystal dimensions 0.50×0.40×0.10 mm^3. Data were measured on a Rigaku RAXIS-RAPID radiation diffractomater with graphite monochromated Mo Kα radiation. Total 24288 reflections were collected, using the ω–2θ scan technique to a maximum 2θ value of 55.0°. The structure was solved by direct methods and refined by a full-matrix least-squares method using SIR92 structure analysis software,[20] with 357

[†] CCDC reference number 243861.

variables and 3617 observed reflections [$I>3.00\sigma(I)$]. The non-hydrogen atoms were refined anisotropically. The weighting scheme $w=4F_o^2[0.500\sigma_c^2(F_o)0.002F_o^2]^{-1}$ gave satisfactory agreement analysis. The final R and Rw values were 0.0410 and 0.1220. The maximum peak and minimum peak in the final difference map were 0.61 and -0.77 e$^-$/Å^3, respectively.

4.7. X-ray structure determination of 12[‡]

Orange prism, $C_{17}H_{21}N_3O_3$, $M=315.37$, orthorhombic, space group $Pna21$, $a=7.1520(2)$ Å, $b=18.7731(5)$ Å, $c=11.4415(3)$ Å, $V=1536.20(7)$ Å^3, $Z=4$, $D_c=1.363$ g mL^{-1}, crystal dimensions $0.80\times0.50\times0.10$ mm^3. Data were measured on a Rigaku RAXIS-RAPID radiation diffractomater with graphite monochromated Mo Kα radiation. Total 13,877 reflections were collected, using the ω–2θ scan technique to a maximum 2θ value of 55.0°. The structure was solved by direct methods and refined by a full-matrix least-squares method using SIR92 structure analysis software,[20] with 230 variables and 1671 observed reflections [$I>3.00\sigma(I)$]. The non-hydrogen atoms were refined anisotropically. The weighting scheme $w=4F_o^2[0.500\sigma_c^2(F_o)+0.0030F_o^2]^{-1}$ gave satisfactory agreement analysis. The final R and R_w values were 0.0440 and 0.1230. The maximum peak and minimum peak in the final difference map were 0.26 and -0.32 e$^-$/Å^3, respectively.

4.7.1. Variable temperature NMR data of 12. Temperature: -90 °C (CD_2Cl_2): ^{1}H NMR (500 MHz) δ 1.02 (3H, t, $J=7.2$ Hz, CH_3), 1.34 (3H, t, $J=7.2$ Hz, CH_3), 3.22 (3H, s, NMe), 3.33 (3H, s, NMe), 3.44–3.53 (2H, m, CH_2), 3.58–3.65 (1H, m, CH_2), 3.71–3.78 (1H, m, CH_2), 6.76 (1H, dd, $J=10.6$, 7.2 Hz, H-3), 6.83 (1H, d, $J=11.6$ Hz, H-5), 7.09 (1H, dd, $J=11.6$, 7.2 Hz, H-4), 7.12 (1H, dd, $J=10.6$, 8.4 Hz, H-2), 8.64 (1H, d, $J=8.4$ Hz, H-1); ^{13}C NMR (125.7 MHz) δ 10.7 (CH_3), 11.3 (CH_3), 26.9 (NCH_3), 27.3 (NCH_3), 44.0 (CH_2), 46.0 (CH_2), 86.2 (C-5), 113.1 (C-7′), 122.7 (C-3′), 124.4 (C-5′), 126.0 (C-2′), 129.8 (C-6′), 133.4 (C-4′), 151.9 (C-2), 160.3 (C-4 or 6), 161.5 (C-4 or 6), 172.6 (C-1′).

4.8. Cyclic voltammetry of 9, 12, and 6b–d$^+\cdot$BF$_4^-$

The reduction potential of **9**, **12**, and **6b–d**$^+\cdot$**BF**$_4^-$ was determined by means of CV-27 voltammetry controller (BAS Co). A three-electrode cell was used, consisting of Pt working and counter electrodes and a reference Ag/$AgNO_3$ electrode. Nitrogen was bubbled through an acetonitrile solution (4 mL) of **9**, **12**, and **6b–d**$^+\cdot$**BF**$_4^-$ (0.5 mmol dm^{-3}) and Bu_4NClO_4 (0.1 mol dm^{-3}) to deaerate it. The measurements were made at a scan rate of 0.1 V s^{-1} and the voltammograms were recorded on a WX-1000-UM-019 (Graphtec Co) X-Y recorder. Immediately after the measurements, ferrocene (0.1 mmol) ($E_{1/2}=+0.083$) was added as the internal standard, and the observed peak potential was corrected with reference to this standard. Compounds **9** and **12** exhibited one irreversible oxidation wave and one irreversible reduction wave. Compounds **6b–d**$^+\cdot$**BF**$_4^-$ exhibited one irreversible reduction wave.

[‡] CCDC reference number 243862.

4.9. General procedure for the autorecycling oxidation of amines catalyzed by 4$^+\cdot$BF$_4^-$, 5$^+\cdot$BF$_4^-$, and 6a,e$^+\cdot$BF$_4^-$ under photo-irradiation

A CH_3CN (16 mL) solution of compounds **4**$^+\cdot$**BF**$_4^-$, **5**$^+\cdot$**BF**$_4^-$, and **6a**,**e**$^+\cdot$**BF**$_4^-$ (0.005 mmol) and amines (2.5 mmol, 500 equiv.) in a Pyrex tube was irradiated by RPR-100, 350 nm lamps under aerobic conditions for the period indicated in Table 5. The reaction mixture was concentrated in vacuo and diluted with Et_2O and filtered. The ^{1}H NMR spectra of the filtrates revealed the formation of the imines (Table 5). The filtrate was treated with a saturated solution of 2,4-dinitrophenylhydrazine in 6% HCl to give 2,4-dinitrophenylhydrazone. The results are summarized in Table 5.

Acknowledgements

Financial support from a Waseda University Grant for Special Research Project and 21COE ‘Practical Nanochemistry’ from MEXT, Japan, is gratefully acknowledged. We thank the Materials Characterization Central Laboratory, Waseda University, for technical assistance with the spectral data, elemental analyses and X-ray analyses.

References and notes

1. Muller, F. *Chemistry and Biochemistry of Flavoenzymes*; Muller, F., Ed.; CRC: Boca Raton, FL, 1991; Vol. 1, pp 1–71 and references cited therein.
2. Hamilton, G. A.; Kaiser, E. T., Kezdy, F. J., Eds.; *Progress in Bioorganic Chemistry*; Vol. 1. Wiley: New York; 1971. p. 83.
3. (a) Chiu, C. C.; Pan, K.; Jordan, F. *J. Am. Chem. Soc.* **1995**, *117*, 7027–7028. (b) Kim, J.; Hoegy, S. E.; Mariano, P. S. *J. Am. Chem. Soc.* **1995**, *117*, 100–105. (c) Murahashi, S.; Ono, S.; Imada, Y. *Angew. Chem. Int. Ed. Engl* **2002**, *41*, 2366–2368. (d) Bergstad, K.; Jonsson, S.; Bächvall, J. *J. Am. Chem. Soc.* **1999**, *121*, 10424–10425. (e) Van Houten, K. A.; Kim, J.; Bogdan, M. A.; Ferri, D. C.; Mariano, P. S. *J. Am. Chem. Soc.* **1998**, *120*, 5864–5872. (f) Zheng, Y.; Ornstein, R. L. *J. Am. Chem. Soc.* **1996**, *118*, 9402–9408. (g) Breinlinger, E. C.; Keenan, C. J.; Rotello, V. M. *J. Am. Chem. Soc.* **1998**, *120*, 8606–8609. (h) Hasford, J. J.; Rizzo, C. J. *J. Am. Chem. Soc.* **1998**, *120*, 2251–2255. (i) Antony, J.; Medvedev, D. M.; Stuchebrukhov, A. A. *J. Am. Chem. Soc.* **2000**, *122*, 1057–1065.
4. Walsh, C. *Acc. Chem. Res.* **1986**, *19*, 216–221 and references cited therein.
5. Yoneda, F.; Tanaka, K. *Med. Res. Rev.* **1987**, *4*, 477–506 and references cited therein.
6. Yoneda, F.; Kokel, B. *Chemistry and Biochemistry of Flavoenzymes*; Muller, F., Ed.; CRC: Boca Raton, FL, 1991; Vol.1, pp 121–169 and references cited therein.
7. Yoneda, F.; Hirayama, R.; Yamashita, M. *Chem. Lett.* **1980**, 1157–1160.
8. Nitta, M.; Tajima, Y. *Synthesis* **2000**, 651–654.
9. Takayasu, T.; Mizuta, Y.; Nitta, M. *Heterocycles* **2001**, *54*, 601–606.
10. Naya, S.; Iida, Y.; Nitta, M. *Tetrahedron* **2004**, *60*, 459–467.

11. Naya, S.; Nitta, M. *Tetrahedron* **2003**, *59*, 3709–3718.
12. Naya, S.; Miyama, H.; Yasu, K.; Takayasu, T.; Nitta, M. *Tetrahedron* **2003**, *59*, 1811–1821.
13. Naya, S.; Miyama, H.; Yasu, K.; Takayasu, T.; Nitta, M. *Tetrahedron* **2003**, *59*, 4929–4938.
14. Naya, S.; Nitta, M. *Tetrahedron* **2003**, *59*, 7291–7299.
15. Naya, S.; Nitta, M. *J. Chem. Soc., Perkin Trans. 2* **2002**, 1017–1023.
16. Dean, J. A. *Lange's Handbook of Chemistry*. 11th ed.; McGraw-Hill: New York, York pp 3-8 and 3-9.
17. Hansch, C.; Leo, A.; Taft, W. *Chem. Rev*. **1991**, *91*, 165–195.
18. Fukuzumi, S.; Kuroda, S. *Res. Chem. Intermed.* **1999**, *25*, 789–811.
19. (a) Jacobi, D.; Abraham, W.; Pischel, U.; Grubert, L.; Schnabel, W. *J. Chem. Soc., Perkin Trans. 2* **1999**, 1241–1248. (b) Jacobi, D.; Abraham, W.; Pischel, U.; Grubert, L.; Stösser, R.; Schnabel, W. *J. Chem. Soc., Perkin Trans. 2* **1999**, 1695–1702.
20. Altomare, A.; Burla, M. C.; Camalli, M.; Cascarano, M.; Giacovazzo, C.; Guagliardi, A.; Polidori, G. *J. Appl. Crystallogr.* **1994**, *27*, 435.